Molecular Crystals
Publication details, including instructions for authors and subscription information:
http://www.tandfonline.com/loi/gmcl15

The luminescence decay of organic scintillators

G. Laustriat [a]

[a] Département de Chimie Nucléaire, Centre de Recherches Nucléaires, STRASBOURG, France

Version of record first published: 21 Mar 2007.

To cite this article: G. Laustriat (1968): The luminescence decay of organic scintillators, Molecular Crystals, 4:1-4, 127-145

To link to this article: http://dx.doi.org/10.1080/15421406808082905

Molecular Crystals, 1968. Vol. 4, pp. 127–145

Printed in Germany

The luminescence decay of organic scintillators

G. LAUSTRIAT

Département de Chimie Nucléaire Centre de Recherches Nucléaires

STRASBOURG (France)

Abstract—Results obtained in the laboratory on the luminescence decay of organic scintillators are reviewed. Theoretical equations, resulting from an analysis of the scintillation process, are shown to be in good agreement with experimental decay curves obtained with crystals and liquid scintillators. The pulse shape discrimination of particles is discussed, and a technique allowing to separate α-particles, protons and β-rays if presented.

1. Introduction

Radioluminescence of aromatic compounds has been extensively used for particle detection since Kallmann discovered, in 1947, organic scintillation counters.[1] For many years, the main advantages of these detectors were found in their very fast response to ionizing particles (10^{-8}–10^{-9} s), and, for liquid scintillators, in the facility of introduction of radioactive materials within the detector.

New interest for these counters arose when it was recognized that the emission decay involves a slow component,[2] the importance of which depends on the ionizing power of the nuclear radiation: this phenomenon was soonly applied to particle dicrimination.[3, 4, 5]

During the last ten years, numerous studies—recently reviewed by Birks[6]—have been devoted to the two components of the scintillation, in order to explain their physical origin and to improve the pulse shape discrimination efficiency.

In general, the fast component is attributed to the emission from excited singlet states induced by charged particles, since the luminescence spectrum and the decay law of the initial part of the scintillation are very similar to those of fluorescence.

The origin of the slow component, by contrast, is less clear and various hypothesis have been made, ascribing the delay of the emission to:

(i) slow ($\sim 10^{-8}$ s) ion-electron recombination;[7]

(ii) triplet-singlet ($T_n \rightarrow S_{n-1}$) intramolecular transition, which could last as long as 10^{-7} s,[8]

(iii) formation of transient metastable pairs of excitons in organic crystals.[9, 10]

These assumptions have been discussed and refuted by Walter,[11] whose experimental data favored the interpretation given by Gervais de Lafond.[12, 13] Following this author, the slow emission results from triplet-triplet interactions leading to singlet states, according to the reaction:

$$T_1 + T_1 \rightarrow S_1 + S_0$$

proposed by Parker and Hatchard[14] to explain the delayed fluorescence of organic substances.

In this paper, we shall give a general review of the main results obtained during the last two years in Strasbourg on the scintillation decay. We shall consider successively:

—chief features of an analysis of the scintillation process made by Voltz,[15] partly in collaboration with T. King[16] at Manchester;

—experimental scintillation decay curves obtained by Walter,[11] Pfeffer[17] and Dupont[18] and their interpretation in the light of the previous theory;

—a discrimination technique set up by Walter and Huck,[19, 20] allowing to separate α particles, protons and β rays, and now currently used in studies of nuclear reactions.

2. The Scintillation process

Emission is the last step of a succession of events, which have to be analysed separately in order to establish the kinetic equations of luminescence.

Spatial distribution of activated species (excitations and ionizations) induced by charged particles

Any charged particle passing through an aromatic medium induces excitation and ionization of molecules, by two types of interactions: distant and central collisions.

Excitations originate only from distant collisions; they occur in a cylindrical zone—the particle track—the radius of which will be denoted r_0.

Ionizations give rise to ions localized in the track, and to secondary electrons. Slow secondaries remain inside the track, where they contribute to enhance the activation density due to the primary particle. Fast secondaries (δ-rays), created by central collisions, leave the track and induce in the medium disseminated activations. Some of them consists of ionizations with liberation of slow electrons which will, in turn, produce activations localized in very small volumes (spherical "spurs"[21] and stretched "blobs".[22]

This schematic picture of the very primary processes (illustrated in Fig. 1) leads us to distinguish, in the medium, two kinds of regions

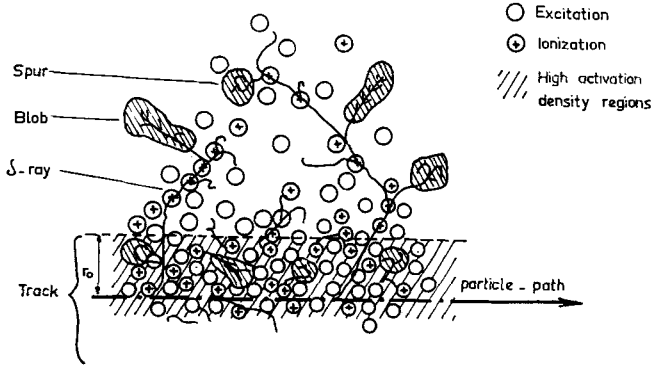

Figure 1. Schematic representation of spatial distribution of activations induced by a charged particle may be suppressed

according to their concentration in activated species:
—track, spurs and blobs (high concentration),
—other regions in the vicinity of the track (low concentration).

It is to be noted that for β-rays, which behave like fast δ-rays, the high concentration region consist of spurs and blobs only.

Nature and evolution of excited states produced by charged particles

Molecular excited states produced by fast charged particles are high energy singlets (S_n) (excited and superexcited,[23]) which are characterized by important transition moments.[15] These levels are created by direct excitation of molecules during distant collisions; excited singlet states may also originate from the recombinations of ions (generated by the particle and its secondaries, or coming from superexcited states).

Other excitations appearing in the scintillator after the passage of the particle are upper triplet states (T_n). Their main source is the ion-electron recombination, which leads mostly (statistically, in 75% of cases) to triplet levels, but they can also be produced directly by inelastic collisions of very slow electrons with the molecules.[24]

The fate of these primary upper excited states S_n and T_n may be different depending on the region in which they were generated:

a) In regions where the activation density is low, interactions between activated species are negligible. Excited molecules are then subject to intramolecular processes, leading either to dissociation (and ionization, for superexcited singlets) or, by internal conversion, to lowest excited states S_1 and T_1.

b) in the track, spurs and blobs, characterised by a high local concentration of activations (S_n, T_n and ions I^+), interactions between the latter are furthermore to be considered. For example, the following processes should be important†:

a) $S_n + S_m \rightarrow S_0 + [I^+ + e^-]$

b) $S_n \xrightarrow{(\mathbf{E})} I^+ + e^-$ ($\mathbf{E}$: electric field due to neighbour ions)

both producing ionizations. Subsequent recombinations lead then mostly upper triplet states T_n, which are subject to the intramolecular transitions mentioned above.

It comes out that, at the end of this sequence of events (summarized in Table 1), a large number of excited molecules are in their lowest triplet state, and that the concentration of these T_1 excitations is high in the track, spurs and blobs (much higher, at least, than in the remainder of the medium). Triplet-triplet interactions may therefore be important in these regions, and the following reactions must be considered:

$$T_1 + T_1 \begin{cases} \xrightarrow{k_{TT}} S_1 + S_0 \\ \xrightarrow{k'_{TT}} T_1 + S_0 \\ \xrightarrow{k''_{TT}} 2S_0 \end{cases}$$

the first of which produces singlet states S_1.

† Another important process is the quenching of excitation by activated species, which is responsible for the dependence of the scintillation yield on the nature of the incoming particle.[15, 25] Such a process, however, is very rapid and does not influence the kinetics of the emission.

TABLE 1 Schematic representation of successive processes leading to lowest energy singlet states

Production of high energy excited states by charged particles

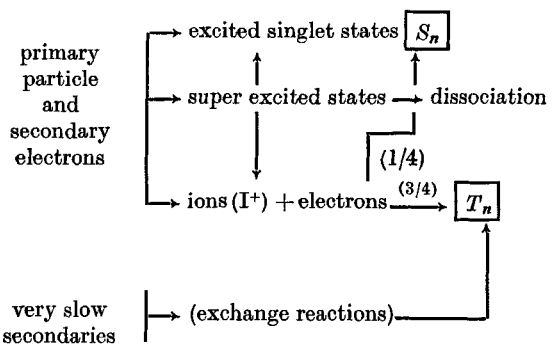

Evolution of high energy excited states

A) *Regions of low activation density*

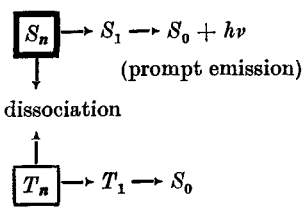

B) *Regions of high activation density (track, spurs and blobs)*

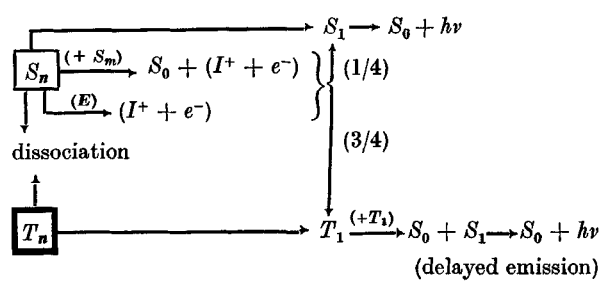

Emission

This analysis leads to the conclusion that, in pure aromatic media (single crystals), the scintillation is due to the radiative deexcitation of singlet states S_1. However, a part of these states is produced very rapidly (by internal conversion $S_n \rightarrow S_1$) and gives rise to a *prompt emission* which is responsible for the fast component, whereas other singlets—issued from triplet-triplet interactions—have a retarded formation, resulting in a *delayed emission* which accounts for the slow component.

In the case of binary systems (liquid and plastic scintillators), the overall process involves the additional step of the energy transfer from S_1 states of the solvent to singlet states (F_1) of the solute (F). For usual concentrations, this reaction is fast enough for the kinetics of the emission not to be modified; however if oxygen is present, an efficient quenching of triplet states T_1 occurs, reducing the delayed emission intensity and modifying its decay law.

Kinetics of luminescence

The very early stages of the scintillation process, leading to the lowest excited states, are too fast to be followed by current experimental techniques. To obtain equations giving the time dependence of intensity, only the kinetics of S_1, T_1 and F_1 states need therefore to be taken in account.

Under these conditions, the prompt emission intensity $I_P(t)$ is found to decay exponentially, with a time constant identical to the mean lifetime τ_S (or τ_F) of the emitting molecules.[15, 16, 18]

For the delayed emission, which is superimposed to the prompt one in the scintillation, the intensity $I_d(t)$ is given by following relationships:

a) pure materials (single crystals):

$$I_d(t) = 2\pi \frac{\eta_s}{\tau_s} k_{TT} \int_0^L dL \int_0^t e^{-\frac{(t-\alpha)}{\tau_s}} d\alpha \int_0^\infty C_T^2(r, \alpha)\, r dr \qquad (1)$$

where: η_S is the quantum yield of fluorescence, L the particle range and $C_T(r, t)$ the local concentration of T_1 states at time t and distance r from the particle path.

For $t \gg \tau_S$, (that is, incidentally, when the prompt emission is over), Eq. (1) assumes a simple asymptotic form:

$$I'_d(t) \simeq \eta_s \frac{N}{[1 + A \ln (1 + t/t_a)]^2 (1 + t/t_a)} \tag{2}$$

where N and A are constants depending on the nature of the scintillator,[15] and t_a a relaxation time defined by:

$$t_a = r_0^2/4D_T \ (D_T\text{: diffusion coefficient of triplet states}).$$

b) Oxygen free liquid scintillators:

Equations (1) and (2) are valid, if we replace τ_S by τ_F and η_S by $\varepsilon_{SF}\eta_F$ to take into account the solvant-solute energy transfer (ε_{SF} is the transfer efficiency and η_F the solute quantum yield). The asymptotic equation then becomes:

$$I'_d(t) = \varepsilon_{SF}\eta_F \frac{N}{[1 + A \ln (1 + t/t_a)]^2 (1 + t/t_a)} \tag{3}$$

c) Oxygen containing liquid scintillators:

Due to the quenching of triplet states by oxygen molecules, the asymptotic equation is different. We have here:

$$I'_d(t) = \varepsilon_{SF}\eta_F \frac{Ne^{-2t/\tau_T}}{\left\{1 + Ae^{t_a/\tau_T}\left[Ei\left(-\frac{t + t_a}{\tau_T}\right) - Ei\left(-\frac{t_a}{\tau_T}\right)\right]\right\}^2 (1 + t/t_a)} \tag{4}$$

where τ_T is the mean life time of T_1 states in the medium, and:

$$Ei(-x) = -\int_x^\infty \frac{e^{-\alpha}}{\alpha} d\alpha$$

The interpretation of the temporal shape of the scintillation, according to the previous analysis is illustrated schematically on Fig. 2:

—for time t such as: $o < t < t_1$, with $t_1 \gg \tau$ ($t_1 = 10\tau$), for instance), the scintillation intensity is the sum of the prompt (curve P) and delayed [curve D, described by Eq. (1)] emissions.

—for $t > t_1$, only the delayed emission is of appreciable importance and decay curve, in this region, is described with a good approximation by Eqs. (2), (3) or (4) depending on the type of the scintillator.

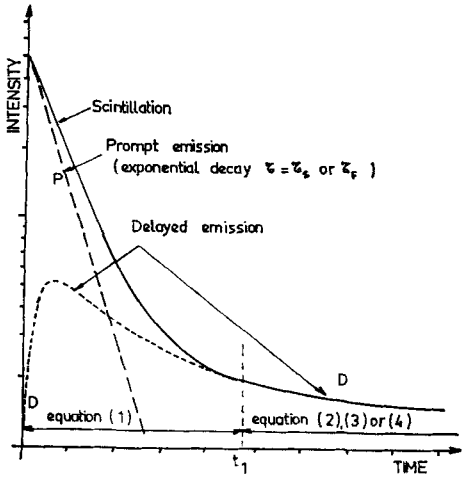

Figure 2. Contributions of the prompt and delayed emissions to the scintillation (schematic).

3. Decay curves of the scintillation

A precise determination of the scintillation decay curves has a double interest:

—practical, for people concerned with pulse shape discrimination;

—theoretical, to verify the analysis of basic processes on which the kinetic equations are based.

Since data are available in the literature on the luminescence decay of crystals, we have set up an apparatus specially designed to work in the nanosecond region, in order to record decay curves of liquid and plastic scintillators [18].

Experimental device

A block diagram of the apparatus is shown in Fig. 3.

The scintillation is viewed by two photomultipliers, one of them (PM 2) giving an electric pulse (A_2) synchronous of the excitation, the other (PM 1) being used as a photon counter and delivering—or not (depending on the light intensity)—a pulse (A_1) due to a single photoelectron.[17]

After differentiation and amplification of Λ_1 and Λ_2, noise is reduced by means of a gate triggered by Λ_2. Both signals (Λ_1 being shaped and Λ_2 delayed by a suitable line) are then sent to the two inputs of a time to pulse height converter, which delivers a pulse (Λ_3) the amplitude of

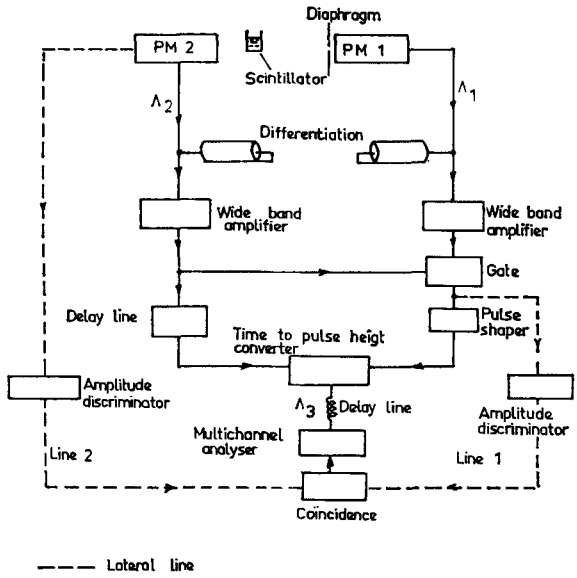

Figure 3. Block diagram of the apparatus used to measure the time dependence of scintillation intensity.

which is proportional to the time interval between arrivals of Λ_1 and Λ_2 to the converter. The distribution curve of the Λ_3 pulse heights, which reproduces the scintillation shape, is finally recorded by a multichannel analyser.

In order to decrease further the contribution of small (noise) pulses, the multichannel analyser is gated by a coincidence unit, receiving pulses transmitted by two amplitude discriminators placed on each line 1 and 2.

Decay times less than one nanosecond can be measured with this device; in the experiments reported here, it was adjusted as to explore the 0–180 ns region.

Results and discussion

(a) Delayed emission

i) *Single crystals.* It has been shown by Voltz[15] and King[16] that the slow component decay curves, obtained with stilbene by Bollinger and Thomas[26] and with anthracene by Wasson[27], could be very precisely interpreted by equation (2). The values of the parameters A and t_a resulting from the adjustment of the theoretical curves to experimental points are: $A = 0.25$ for both crystals, and $t_a = 80\ 10^{-9}$ s for stilbene and $t_a = 40\ 10^{-9}$ s for anthracene.

ii) *Deaerated solutions.* Radioluminescence decay of various liquid scintillators has been studied with the apparatus described above. On Fig. 4 are shown experimental results obtained, under $\alpha(^{210}\text{Po})$ and γ (^{60}Co) excitations, with solutions of terphenyl, PPD† and PBD† in degassed toluene. Solutes were chosen in order to avoid excimer formation,

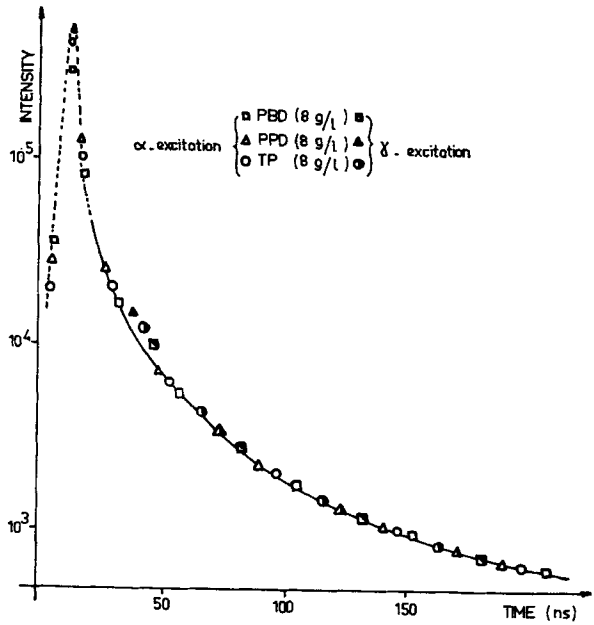

Figure 4. Luminescence decay of liquid scintillators (solvent: degassed toluene).[18] Experimental points normalised at 180 ns. Theoretical curve: Eq. (3).

† PPD = diphenyl-2,5-oxadiazole; PBD = phenyl-2-biphenyl-5-oxadiazole.

which would introduce an additional fluorescence slow component. It appears that: (i) the decay law of the slow emission does not depend on the solute, neither on the particle type—in agreement with the preceding description of the processes, (ii) the theoretical curve, given here by Eq. (2)—using $A = 2$ and $t_a = 2\ 10^{-9}$ s—, fits the experimental point with a good accuracy.

iii) *Oxygenated Solutions.* The oxygen effect on the scintillation decay is illustrated in Fig. 5, which presents results obtained with one of the previously tested solutions (toluene–PDB), saturated with argon, air or oxygen and excited by α-particles (the decay law of the slow component was the same under γ excitation).

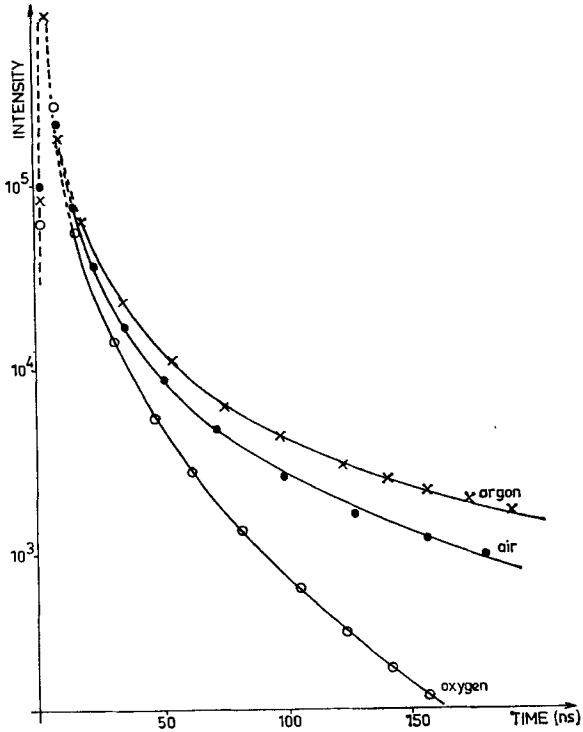

Figure 5. Influence of dissolved oxygen on the decay curve of a liquid scintillator (PBD (8 g/l)—toluene; α-excitation).[18] Experimental points normalized at the intensity maximum. Theoretical curves: equations 3 (argon) and 4 (air, oxygen).

The quenching effect of oxygen on the delayed emission appears very clearly, According to the theory, this effect reduces the mean life time τ_T of triplet states, the values of A and t_a being unaffected by the presence of the gas. Solid curves are given by equation (4), taking for A and t_a the same values as for degassed solutions and $\tau_T = 0.3\mu s$ (or $0.12\ \mu s$) for air (or oxygen) saturated scintillators.[18] Here again the agreement between theory and experiment is quite good.

iv) *Plastic scintillators.* The experimental decay curves obtained with two plastic scintillators are indicated Fig. 6. The interpretation of these results by the previous equations was not found to be satisfactory and requires further work which is currently in progress.

(b) Prompt emission

The temporal shape of the prompt emission can be obtained by subtracting, from the scintillation decay curve, the curve representing the

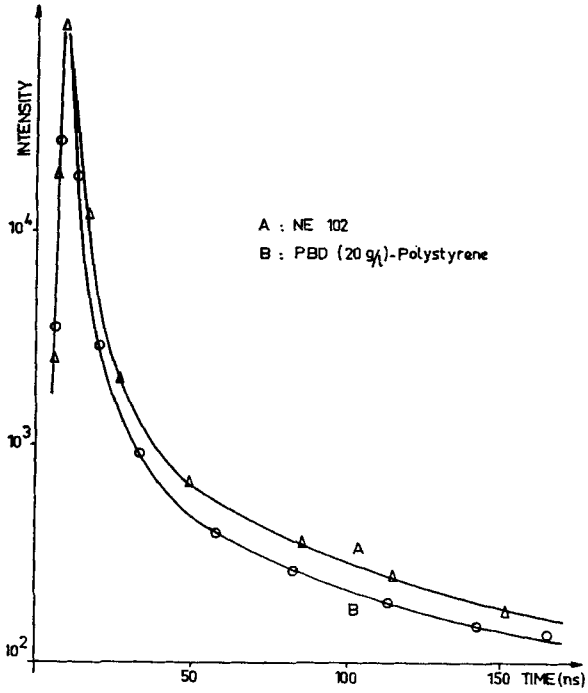

Figure 6. Decay curves of plastic scintillators (α-excitation). Experimental curves, normalized at the intensity maximum.[30]

time dependence of the delayed emission in its initial part (curve D, on Fig. 2, which can be calculated using Eq. (1)—or more precisely its differential expression[15]). The results of this operation is shown, on Fig. 7, in the case of a degassed solution of PBD in toluene. It is seen that, as predicted, the decay curve obtained is exponential, with a time constant very close to the mean life time of the emitting molecules.

(c) Relation between the prompt and delayed emissions and the two components of the scintillation

If both prompt and delayed emissions have decay laws which are independent on the type of the ionizing radiation, their integrated intensities (hereafter denoted as L_p and L_d respectively) depend markedly, by contrast, on the stopping power $\frac{dE}{dx}$ and the charge of the incoming

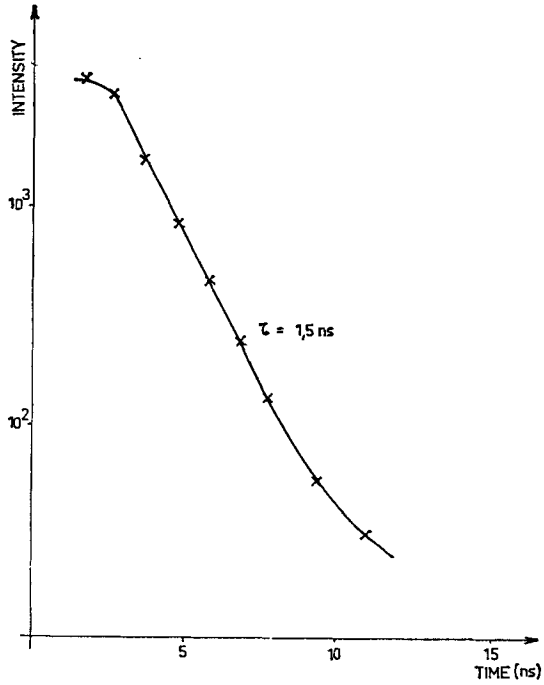

Figure 7. Calculated prompt emission decay curve (γ-excitation). Scintillator: PBD (8 g/l)—benzene ($\tau_F = 1.4$ ns).[18]

particle†. As a result, total amounts of light emitted in the initial part of the scintillation (fast component, F) and in the slow variation region (slow component, S) vary with the type of particles: this is the well known basis of particle discrimination techniques.

However, values of F and S depend on the time t_0 which is arbitrarily chosen as a separation limit between the two components. According to the theory, we have:

$$F = \int_0^{t_0} (I_p + I_d)\, dt$$

$$S = \int_{t_0}^{t_1} (I_p + I_d)\, dt$$

t_1 denoting the time—large but not infinite—up to which the measurement of S is experimentally extended.

The proportion P of light emitted in the slow component $\left(P = \dfrac{S}{F+S}\right)$ is then a function of t_0, and Voltz[15] has shown that the ratio $R(t_0)$, defined as:

$$R(t_0) = \frac{P(t_0)}{G(t_0) - G(t_1)} \quad \text{where } G(t) = 1 + A \ln (1 + t/t_a)$$

should decrease, for increasing values of t_0, to a constant value R_{lim} given by:

$$R_{\text{lim}} = \frac{1}{L_p/L_d[1 - G(t_1)]}$$

From the value of R_{lim}, which can be obtained by analysing the decay curve, it is then possible to estimate L_p/L_d. This ratio has been determined by Voltz,[15] using data of Bollinger and Thomas[26] for a stilbene crystal submitted to various particles; following values has been found:

$(L_p/L_d)_\gamma \simeq 6.5$ (γ rays from ^{60}Co)

$(L_p/L_d)_n \simeq 1.2$ (fast neutrons from a Ra–Be source)

$(L_p/L_d)_\alpha \cong 0.6$ (α rays from ^{244}Cm)

† This phenomenon has been studied in this laboratory by Voltz, Pfeffer and Lopes da Silva[15, 25, 28] who have shown this effect to be mainly due to initial quenching of upper excited states in regions of high excitation density.

These results show that, in the case of γ excitation, most of the light is emitted in the prompt emission, while with α-particles, the greatest fraction of the light originates from the delayed emission.

4. Application to pulse shape discrimination

Particle discrimination is currently used in the laboratory for studying nuclear reactions induced inside the scintillator on carbon nuclei.[19, 20, 29] We shall report here the principle of the apparatus and few typical results which can be obtained.

Apparatus

A circuit has been designed to produce, for each scintillation, two different pulses, the amplitudes of which are proportional to the intensities of the fast (F) and the slow (S) components.[20]

A diagram of the experimental set-up is given in Fig. 8. The detector consists of a stilbene crystal (0.6 cm thick by 2.5 cm diam.) attached to a Dario 56 UVP photomultiplier.

"F" pulses originate from the last dynode and are fed through a stretcher to one imput of the 2-parameters multichannel analyser (64 $\times$ 64 channels).

In order to get "S" pulses, the anode is connected to a circuit composed of a diode (D_1) and of a resistor (R_1). During the first part of the scintilla-

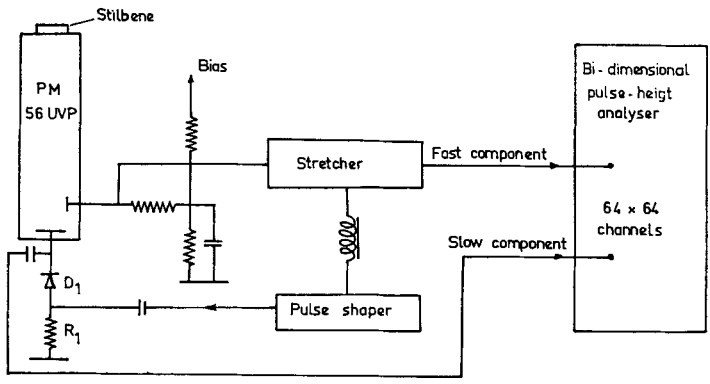

Figure 8. Block diagram of the apparatus used for particle discrimination.

tion, the forward resistance of D_1, added to R_1, is low and the voltage across the load reproduces the decay of luminescence without integration. At a time t_0 after the beginning of the emission, a pulse issued from the strecher turns off the diode up to the time t_1; the resulting high impedance of the load enables to integrate the anode current related to the slow component during the time interval $t_1 - t_0$. The corresponding voltage pulse is then fed to the second input of the analyser.

On the analyser oscilloscope (Fig. 9), each scintillation is then recorded by the vertical displacement (Z axis) of a point, the coordinates (x and y) of which are proportional to the amounts of light emitted in the slow and fast components ($x = k_1 S$, $y = k_2 F$).

Performances and results

In such diagrams, counts corresponding to monokinetic particles of a given type (i.e. of constant F and S) appear at the same place and give rise to a peak. Polykinetic particles (β-rays, recoil protons) characterised by different F and S but a nearly constant† F/S ratio, give rise to an approximately linear deformation of the (x, y) plane, the slope of the line depending on the type of the particles (the higher the ionizing power, the smaller the slope) (Fig. 9).

Figure 10 show experimental results obtained when the stilbene crystal is irradiated by neutrons of different energies (15, 16 and 17 MeV). Three types of particles are clearly separated. —

—Compton electrons, produced by the γ back-ground,

—recoil protons resulting from elastic collisions of neutrons with hydrogen atoms,

—alpha particles of various energies, identified as reaction products of $^{12}C(n, \alpha)\,^{9}Be$ and $^{12}C(n, n')\,3\alpha$. The energy of emitted alphas is shown to increase with neutron energy, accordingly to the kinematics of these reactions.

† It has been shown by Walter[5] that F, by contrast to S, is not a linear function of the energy (this appears on Figure 12, where the lines corresponding to electrons and protons present a slight curvature). For that reason, the particle discrimination is less accurate with an analog device than with a bidimensial analyser.

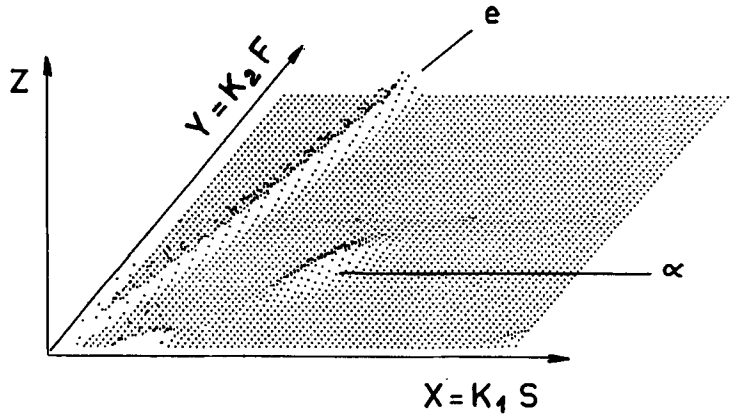

Figure 9. Figure displayed on the two-parameters analyser oscilloscope. The peak corresponds to 8.78 MeV α-particles (^{212}Po) and the line to Compton electrons (γ-rays from ^{208}Tl, ^{212}Pb, ^{212}Bi).

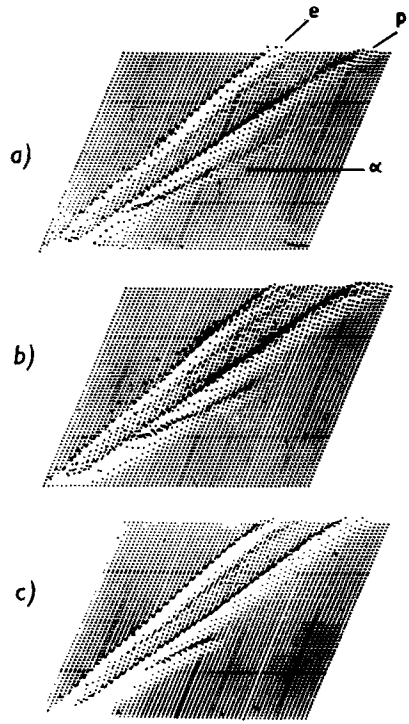

Figure 10. Separation of particles observed when a stilbene crystal is irradiated by fast neutrons. Energy of neutrons: a) 15 MeV; b) 16 MeV; C) 17 MeV.

Two general comments can be made on this technique:

a) usual n-γ discrimination devices do not allow sparation of alphas from recoil protons. Results presented here indicate that α emission is important and may cause serious errors if not taken in consideration.

b) The energy distribution of the incoming particle can be determined by using either "F" or "S" pulses only. The energy resolution is about the same in the two cases. However, the use of the "S" pulses for neutron energy measurements is of particular interest since a linear relationship is observed between the amount of light emitted in the slow component and the energy of the particle, while this is not the case for the fast component.[5]

5. Conclusion

Besides its interest for pulse shape discrimination techniques, the knowledge of radioluminescence decay curves is, in itself, of fundamental importance in radiation physics and chemistry. In effect, by giving the possibility to verify the decay laws derived from theoretical considerations, it enables to get informations on the nature of the basic processes induced by nuclear particles in organic media. For instance, the agreement, found in this work, between decay curves and kinetic equations give an experimental evidence that bimolecular interactions between some activated species (most probably molecules excited in their lowest triplet level) leading to delayed singlet states occur efficienctly in high activation density regions (track, spurs, blobs). Furthermore, numerical values of the adjustable parameters included in theoretical equations may be of interest. For example, from the value of t_a, it is possible to estimate the track radius r_0 ($r_0 = 2\sqrt{D_1 t_a}$) in aromatic solvents, since in liquids the diffusion coefficient of triplet states (D_1) is the same as the diffusion coefficient (D_s) of molecules†.

Further informations on primary processes (mean distance between activations in the track, energy required to form a quenching center) are expected from radioluminescence efficiency and decay measurements with very thin scintillators.

† Taking $D_T \simeq D_S \simeq 2.2\ 10^{-5}\ \mathrm{cm^2\ s^{-1}}$, and $t_a \simeq 2\ 10^{-9}\mathrm{s}$ (found in this work for benzene and toluene), one obtains: $r_0 \simeq 50$ Å.

REFERENCES

1. Kallmann, H., *Natur und Technik*, July 1947.
2. Jackson, J. A. and Harrison, F. B., *Phys. Rev.*, **89**, 322, 1953.
3. Owen, R. B., IRE *Trans. Nucl. Sci.* NS-**5**, 198, 1958; Nucleonics, **17**, n^0 9, 22, 1959.
4. Brooks, F. D., *Nucl. Instr. Meth.*, **4**, 151, 1959.
5. Walter, G. and Coche, A., *J. Physique Rad.*, **22**, 165, 1961.
6. Birks, J. B., *The Theory and Practice of Scintillation Counting*, Chapt. 6, Pergamon Press, Oxford 1964.
7. Buck, W. L., *IRE Trans. Nucl. Sci.*, NS-**7**, 11, 1960.
8. Birks, J. B., *IRE Trans. Nucl. Sci.*, NS-**7**, 2, 1960.
9. Northrop, D. C. and Simpson, O., *Proc. Roy. Soc.*, A **234**, 124, 1956; ibid, A **244**, 377, 1958.
10. Gibbons, P. E., Northrop, D. C. and Simpson, O., *Proc. Phys. Soc.*, **79**, 373, 1962.
11. Walter, G., Thèse, Strasbourg, (1964).
12. Gervais de Lafond Y., Thèse, Toulouse, (1962).
13. Blanc, D., Cambou, F., and Gervais de Lafond, Y., *J. Physique*, **25**, 319, 1964.
14. Parker, C. A. and Hatchard, C. G., *Trans. Far. Soc.*, **57**, 1894, 1961; *Proc. Roy. Soc.*, A **269**, 574, 1962.
15. Voltz, R., Thèse, Strasbourg, (1965).
16. King, T. A. and Voltz, R., *Proc. Roy. Soc.*, A **289**, 424, 1966.
17. Pfeffer, G., Thèse, Strasbourg, (1965).
18. Dupont, H., Thèse, Strasbourg, (1966).
19. Walter, G., Huck, A., Trevetin, J. P. and Coche, A., *J. Physique*, **24**, 1017, 1963.
20. Walter, G., Huck, A., Gonidec, J. P. and Coche, A., *Onde Electrique*, **346**, 553, 1964.
21. Samuel, A. H. and Magee, J. L., *J. Chem. Phys.*, **21**, 1080, 1953.
22. Magee, J. L., Funabashi, K. and Mozumder, A., *Proceedings of the 6th. Japan Conference on Radioisotopes*, p. 755, 1964.
23. Platzman, R. L., *J. Physique Rad.*, **21**, 853, 1960; *Rad. Res.*, **17**, 419, 1962.
24. Massey, H. S. W. and Burhop, E. H. S., *Electronic and Ionic Impact Phenomena*, Oxford, 1962.
25. Voltz, R., Lopes da Silva J., Laustriat, G. and Coche, A., *J. Chem. Phys.*, **45**, 3306, 1966.
26. Bollinger, L. M. and Thomas, G. E., *Rev. Sci. Instr.*, **32**, 1044, 1961.
27. Wasson, M. M., Memo, M. 1153, Aere, Harwell, 1962.
28. Voltz, R., Pfeffer, G., Lopes da Silva, J., and Laustriat, G., *International Symposium on Luminescence*, Munich, 1965.
29. Huck, A., Walter, G., and Coche, A., *J. Physique*, (in press).
30. Dupont, H., Pfeffer, G., Laustriat, G. and Coche, A., *Nucl. Instrum. Meth.*, **47**, 93, 1967.